

# Experimental investigation of the Soret effect in acetone/water and dimethylsulfoxide/water mixtures

Hui Ning<sup>1,\*</sup> and Simone Wiegand<sup>1,†</sup>

<sup>1</sup>*Forschungszentrum Jülich GmbH,  
IFF - Weiche Materie, D-52428 Jülich, Germany*

(Dated: November 4, 2006)

## Abstract

The thermal diffusion behavior of acetone/water and dimethylsulfoxide(DMSO)/water mixtures has been experimentally investigated by a transient holographic grating technique named thermal diffusion forced Rayleigh scattering (TDFRS). For both systems a sign change of the Soret coefficient  $S_T$  with varying water content has been predicted by simulations [C. Nieto Draghi *et al.*, J.Chem.Phys. **122**, 114503(2005)]. The sign change of  $S_T$  is confirmed by the experiment. Except for equimolar concentrations of acetone/water the agreement between the experimental and simulation data is reasonable.

PACS numbers:

## I. INTRODUCTION

A temperature heterogeneity in a fluid mixture induces a mass flux, which results in a concentration gradient. This effect is known as Ludwig-Soret effect.<sup>1,2</sup> For a binary mixture in a temperature gradient  $\nabla T$ , the enrichment of one component  $\nabla x$  is characterized by the Soret coefficient  $S_T$ , as

$$S_T = -\frac{1}{x(1-x)} \frac{|\nabla x|}{|\nabla T|}. \quad (1)$$

A positive Soret coefficient of the component with the molar fraction  $x$  implies that this component moves to the colder region of the fluid.<sup>3,4</sup> Although the Ludwig-Soret effect had been discovered 150 years ago, there is still no microscopic understanding for the effect in fluid mixtures.<sup>5</sup>

In the past the thermal diffusion behavior of simple fluid mixtures has been studied extensively.<sup>6-13</sup> Organic liquid mixtures have been used in a benchmark test, to establish reference data.<sup>14</sup> Recently, special focus has been on the dependence of  $S_T$  on parameters such as mass and moment of inertia.<sup>6,11,12</sup> For many associating liquids, where specific interactions such as hydrogen-bonding or electrostatic interactions exist, sign changes of  $S_T$  with composition have been observed.<sup>6,9,15,16</sup>

Molecular dynamics (MD) simulations have become an important tool in the investigation of thermal diffusion behavior of Lennard-Jones model fluids and small-molecule liquids.<sup>17-21</sup> Lately, the simulation techniques for non-equilibrium properties have been improved, which have led to a reasonable agreement between simulations and experiments for associating and non-associating liquid mixtures.<sup>21-23</sup> Simulations and also a two-chamber lattice model calculation have shown that the relation between the cross interactions and the pure interactions determine whether the sign of the Soret coefficient changes with concentration.<sup>23-25</sup> Nieto-Draghi *et al.*<sup>26</sup> also predicted a sign change for the associating liquid mixtures acetone/water and dimethyl sulfoxide(DMSO)/water, which so far has not been confirmed by experiments.

In the present paper we investigate the Soret coefficient of acetone and DMSO in water for different concentrations by thermal diffusion forced Rayleigh scattering (TDFRS). The experimental results are compared with the recently published simulation data and the influence of different parameters such as the hydrogen-bond capability, mass and moment of inertia are discussed.

## II. EXPERIMENT

### A. Sample preparation

Acetone (Laborchemie Handels-GmbH, purity > 99.9%), and DMSO (Sigma-Aldrich, purity  $\geq 99.9\%$ ) were used without further purification. We took deionized water (Milli-Q). The mixtures were prepared as follows: First a very small amount (roughly  $10^{-6}\text{wt}\%$ ) of the dye basantol yellow,<sup>27</sup> was dissolved in the solvents. For each solution the optical density was adjusted to  $2\text{--}3\text{ cm}^{-1}$  at a wavelength of  $\lambda = 488\text{ nm}$ . Samples for the TDFRS measurements were prepared just before the measurement to avoid evaporation. The solutions were directly filtered into the sample cells (Spartan,  $0.45\text{ }\mu\text{m}$ ). The temperature was controlled by a circulating water bath and all measurements were performed at  $T = 298 \pm 0.02\text{ K}$ .

### B. Data analysis and set-up

The thermal diffusion behavior of the solutions was investigated by thermal diffusion forced Rayleigh scattering (TDFRS). A detailed description of the set-up can be found elsewhere.<sup>27</sup> In brief, a grating is created by the interference of two laser beams ( $\lambda = 488\text{ nm}$ ). A tiny amount of inert dye, which has a strong absorption band at  $\lambda = 488\text{ nm}$ , converts the optical grating into a temperature grating. Both the temperature grating and the resulting concentration grating contribute to the refractive index grating, which is read out by the diffraction of a third laser beam ( $\lambda = 633\text{ nm}$ ). The time dependent heterodyne diffraction signal  $\zeta_{\text{het}}$  is evaluated by the equation,

$$\zeta_{\text{het}}(t) = 1 + \left(\frac{\partial n}{\partial T}\right)^{-1} \left(\frac{\partial n}{\partial x}\right) S_{\text{T}} x (1 - x) \left(1 - e^{-q^2 D t}\right), \quad (2)$$

with the refractive index increment with concentration at constant pressure and temperature ( $\partial n/\partial x$ ), the derivative of the refractive index with temperature at constant pressure and concentration ( $\partial n/\partial T$ ), the grating vector  $q$  and the collective diffusion coefficient  $D$ .

### C. Refractive index increments

The refractive indices of the mixtures were measured with an Abbe refractometer. The refractive index increment ( $\partial n/\partial x$ ) was determined from the derivative of a fifth order poly-

nomial fit of the refractive index data. We used the molar fraction of the organic solvent (acetone or DMSO) as concentration variable.  $(\partial n/\partial T)$  was directly measured by an interferometer. The contrast factors  $(\partial n/\partial x)$  and  $(\partial n/\partial T)$  are shown in Fig.1 and 2, respectively. For the acetone/water mixture, the slope of the refractive index  $n$  changes from positive to negative at  $x_{\text{acetone}} = 0.4$ , while  $(\partial n/\partial x)$  of DMSO/water constantly decreases with DMSO concentration. The increment  $(\partial n/\partial T)$  of both solutions decreases with decreasing water content.

### III. RESULTS AND DISCUSSION

For both aqueous solutions we performed TDFRS measurements in the entire concentration range. In Fig.3 the Soret coefficient  $S_T$  is shown as a function of the molar fraction of acetone and DMSO, respectively. In the water-rich region the Soret coefficient  $S_T$  of acetone decreases with increasing acetone concentration and reaches a minimum at a molar fraction of  $x_{\text{acetone}} = 0.5$ . For higher acetone concentrations ( $x_{\text{acetone}} > 0.5$ )  $S_T$  increases with  $x_{\text{acetone}}$ . Typically, the error bars do not exceed the symbol size, but for concentrations around  $x_{\text{acetone}} = 0.5$  the uncertainties became larger due to the low value of the refractive index increment  $(\partial n/\partial x)$ , which leads to a small amplitude of the concentration part of the TDFRS-signal (cf. Eq. 2). The Soret coefficient of DMSO in water decreases with DMSO concentration and reaches almost a plateau or wide minimum for  $x_{\text{DMSO}} > 0.6$ . Both systems show a sign change of Soret coefficient with concentration. Similar to other aqueous solutions such as methanol/water<sup>16</sup> and ethanol/water,<sup>8,9,28,29</sup> the sign change occurs in the water rich region at approximately  $x_{\text{acetone}} = 0.11$  for acetone and around  $x_{\text{DMSO}} = 0.2$  for DMSO.

In Fig.3, we plot the simulation data obtained by boundary driven reverse non-equilibrium MD by Rousseau *et al.*,<sup>23,26</sup> which are also obtained at ambient temperature and pressure. Also the simulations results show a sign change from positive to negative with decreasing water content. Compared to the experimental results the simulations predict the sign change at a slightly lower water content. However, in the case of DMSO it is hard to decide, where the sign change occurs, since there are very few simulation data around the sign change concentration. For acetone/water mixtures (in Fig.3a), the simulation data are consistent with experimental data for the high and low water content. The minimum of the

Soret coefficient around  $x_{\text{acetone}} = 0.5$  is not reproduced in the simulations. For the system DMSO/water (in Fig.3b), the simulation data agree with our experimental data within the error bars for molar fractions  $x_{\text{DMSO}}$  above 0.3, while in the water-rich regime the simulation data overestimate the experimental data by a factor of four.

Acetone and DMSO show similar molecular structures. While the central atom of acetone is carbon, it is sulphur in the case of DMSO. Compared to acetone DMSO has a larger mass, size, dipole moment and moment of inertia (compare Tab. I). In order to explore this effect we have calculated the moments of inertia about the symmetry axis using an atomistic model for single molecules in vacuum.<sup>30</sup> For comparison we used the highest moment of inertia along the z-axis. Comparing the parameters for the two systems it is not understood, why  $S_T$  of acetone in water shows such a pronounced minimum for equimolar mixtures.

Recently, Köhler and co-workers<sup>6</sup> postulate that the Soret coefficient can be written as a sum of three contributions:

$$S_T = a_M \Delta M + b_I \Delta I + S_T^0. \quad (3)$$

where  $\Delta M = M_1 - M_2$  and  $\Delta I = I_1 - I_2$  are the absolute difference in mass and moment of inertia of the two components, respectively. The third contribution,  $S_T^0$ , reflects the chemical differences of the molecules. It is difficult to apply this equation to associating fluids because they show a rather pronounced concentration dependence in contrast to non-associating liquids.<sup>7</sup> Furthermore, the chemical contribution will be quite different indicated by difference in properties such as the hydrogen-bond capability and dipole moment. Further we list in Table I also the Hildebrand solubility parameter  $\delta$ , which represents a thermodynamic property of materials which implies the enthalpy change on mixing or the energy associated with the net attractive interactions of the material. A correlation between the Soret coefficient and the cohesive energy or Hildebrand parameter is quite intuitive and has been carried out in the past.<sup>5,31-33</sup> It is reasonable to expect that a larger difference of the Hildebrand parameters between the two components of fluid, which implies a low compatibility, leads to a larger Soret coefficient. For the listed systems the largest difference in  $\delta$  occurs for acetone and water, which shows also the largest magnitude of  $S_T$ . For the other systems we find no obvious correlation, but the differences in  $\delta$  are not very pronounced and depend on the determination methods.<sup>34-36</sup> The four aqueous systems listed in Table I show a similar trend. For high water content the water molecules migrate to the warm side, while for lower water content the migration is reversed (cf. Fig. 4). This implies that only in the

case of high water content the heavier component moves to the cold side. With increasing water content the Soret coefficient decays linearly, changes sign between  $x_{\text{solvent}} = 0.1 - 0.2$ , and passes through a more or less shallow minimum and reaches a final or plateau value. The sign change concentration  $x_{\text{solvent}}^{\pm}$  of the first three systems shows a linear correlation with the Hildebrandt parameter  $\delta$  as it also has been observed in simulations for Lennard-Jones fluids,<sup>32</sup> but the system DMSO deviates from the other systems. On the other hand the concentration dependence of  $S_T$  for DMSO is similar to methanol and ethanol, while acetone shows an unusual dependence on the composition with a pronounced minimum.

The two studied systems here belong to the class of associating systems. For those mixtures an additional complexity arises from the presence of hydrogen-bonding which often enhances excess quantities compared to non-associating mixtures.<sup>37</sup> Lattice simulations,<sup>23</sup> lattice calculations<sup>24</sup> and also recent simulations<sup>25</sup> show that the pronounced concentration dependence of those mixtures is strongly related to the cross interactions. If the cross interaction of the two components is stronger than the average value of the pure components, the minority component accumulates always on the cold side. Finally, we would like to point out that the concentration  $x_{\text{solvent}}^{\text{hyd}}$ , where the hydrogen-bond network breaks down by addition of a second component (cf. Table I) correlates with the concentration  $x_{\text{solvent}}^{\pm}$ , where the Soret coefficient changes sign.<sup>38-40</sup> This observation has also been made for the Soret coefficient of poly(ethylenoxide) in the solvent mixture ethanol/water, which changes sign at  $x_{\text{ethanol}} = 0.08$ .<sup>29</sup> This indicates that thermal diffusion is quite sensitive to changes in the fluid structure.

#### IV. CONCLUSION

In this paper, we have presented Soret coefficients for acetone and DMSO in water. The Soret effect of both systems shows a strong dependence on the composition. Similar to other associating systems, like methanol/water and ethanol/water, we found that Soret coefficient of non-water component of the studied mixtures decreases with decreasing water content and changes sign, when the molar fraction of the non-aqueous component is between 10% and 20%. For all studied aqueous systems the sign change composition is correlated with the composition where the hydrogen-bond network breaks down due to addition of a second component. This change in the local structure of the fluid mixture results in a distinct

change of the chemical contribution  $S_T^0$  to the Soret coefficient and leads depending on the size of the mass and moment of inertia contributions eventually to a sign change of the total Soret coefficient  $S_T$ . The data for acetone show the most pronounced minimum, while the other three systems behave very similar. With the exception of the pronounced minimum of  $S_T$  for equimolar mixture of acetone/water our experimental data compare well with the previously published simulation data.

### **Acknowledgments**

The authors would like to thank Hartmut Kriegs and Pavel Polyakov for their experimental assistance. We thank Malte Kleemeier and Mathieu McPhie for carefully reading the manuscript. This work was partially supported by the Deutsche Forschungsgemeinschaft grant Wi 1684.

- 
- \* [h.ning@fz-juelich.de](mailto:h.ning@fz-juelich.de); <http://www.fz-juelich.de/iff/personen/H.Ning/>
- † [s.wiegand@fz-juelich.de](mailto:s.wiegand@fz-juelich.de); <http://www.fz-juelich.de/iff/personen/S.Wiegand/>
- <sup>1</sup> C. Ludwig, Sitz. ber. Akad. Wiss. Wien Math.-naturw. Kl **20**, 539 (1856).
  - <sup>2</sup> C. Soret, Arch. Geneve **3**, 48 (1879).
  - <sup>3</sup> A. Firoozabadi, K. Ghorayeb, and K. Shukla, AIChE Journal **46**, 892 (2000).
  - <sup>4</sup> S. Wiegand and W. Köhler, in *Thermal Nonequilibrium Phenomena in Fluid Mixtures* (Springer, Berlin, 2002), vol. LNP584, pp. 189–210.
  - <sup>5</sup> S. Wiegand, J.Phys.:Condens. Matter **16**, R357 (2004).
  - <sup>6</sup> G. Wittko and W. Köhler, J. Chem. Phys. **123**, 014506 (2005).
  - <sup>7</sup> W. Köhler and B. Müller, J. Chem. Phys. **103**, 4367 (1995).
  - <sup>8</sup> J. F. Dutrieux, J. K. Platten, G. Chavepeyer, and M. M. Bou-Ali, J. Phys. Chem. B **106**, 6104 (2002).
  - <sup>9</sup> P. Kolodner, H. Williams, and C. Moe, J. Chem. Phys. **88**, 6512 (1988).
  - <sup>10</sup> O. Ecenarro, J. A. Madariaga, J. Navarro, C. M. Santamaria, J. A. Carrion, and J. M. Saviron, J. Phys.-Cond. Matt. **2**, 2289 (1990).
  - <sup>11</sup> C. Debuschewitz and W. Köhler, Phys. Rev. Lett. **87**, 055901 (2001).
  - <sup>12</sup> P. Polyakov and S. Wiegand, Proc. 7th international meeting on thermodiffusion San Sebastian pp. 399–407 (2006).
  - <sup>13</sup> M. M. Bou-Ali, O. Ecenarro, J. A. Madariaga, C. M. Santamaria, and J. J. Valencia, Phys. Rev. E **62**, 1420 (2000).
  - <sup>14</sup> J. K. Platten, M. M. Bou-Ali, P. Costeseque, J. F. Dutrieux, W. Köhler, C. Leppla, S. Wiegand, and G. Wittko, Philos. Mag. **83**, 1965 (2003).
  - <sup>15</sup> I. Prigogine, L. Debrouckere, and R. Amand, Physica **16**, 851 (1950).
  - <sup>16</sup> L. J. Tichacek, W. S. Kmak, and H. G. Drickamer, J. Phys. Chem. **60**, 660 (1956).
  - <sup>17</sup> B. Hafskjold, in *Thermal nonequilibrium phenomena in fluid mixtures*, edited by W. Köhler and S. Wiegand (Springer, Heidelberg, 2002), Lecture Notes in Physics, pp. 3–23.
  - <sup>18</sup> P. Bordat, D. Reith, and F. Müller-Plathe, J. Chem. Phys. **115**, 8978 (2001).
  - <sup>19</sup> G. Galliero, B. Duguay, J. P. Caltagirone, and F. Montel, Fluid Phase Equilib. **208**, 171 (2003).
  - <sup>20</sup> A. Perronace, G. Ciccotti, F. Leroy, A. H. Fuchs, and B. Rousseau, Phys. Rev. E **66**, 031201



- (2002).
- <sup>21</sup> M. M. Zhang and F. Müller-Plathe, J. Chem. Phys. **123**, 124502 (2005).
  - <sup>22</sup> A. Perronace, C. Leppla, F. Leroy, B. Rousseau, and S. Wiegand, J. Chem. Phys. **116**, 3718 (2002).
  - <sup>23</sup> B. Rousseau, C. Nieto-Draghi, and J. Bonet Avalos, Europhys. Lett. **67**, 976 (2004).
  - <sup>24</sup> J. Luettmer-Strathmann, Int. J. Thermophys. **26**, 1693 (2005).
  - <sup>25</sup> M. M. Zhang and F. Müller-Plathe, J. Chem. Phys. (2006), accepted.
  - <sup>26</sup> C. Nieto-Draghi, J. B. Avalos, and B. Rousseau, J. Chem. Phys. **122**, 114503 (2005).
  - <sup>27</sup> H. Ning, R. Kita, H. Kriegs, J. Luettmer-Strathmann, and S. Wiegand, J. Phys. Chem. B **110**, 10746 (2006).
  - <sup>28</sup> K. J. Zhang, M. E. Briggs, R. W. Gammon, and J. V. Sengers, J. Chem. Phys. **104**, 6881 (1996).
  - <sup>29</sup> R. Kita, S. Wiegand, and J. Luettmer Strathmann, J. Chem. Phys. **121**, 3874 (2004).
  - <sup>30</sup> *Chem3D, Ver. 10*, CambridgeSoft, Cambridge, MA (2006).
  - <sup>31</sup> J. Demichowicz-Pigoniowa, M. Mitchell, and H. Tyrrell, J. Chem. Soc. A - Inorg. Phys. Theor. **2**, 307 (1971).
  - <sup>32</sup> D. Reith and F. Müller-Plathe, J. Chem. Phys. **112**, 2436 (2000).
  - <sup>33</sup> E. P. C. Mes, W. T. Kok, and R. Tijssen, International Journal of Polymer Anal. Charact. **8**, 133 (2003).
  - <sup>34</sup> A. F. M. Barton, in *CRC Handbook of Solubility Parameters and Other Cohesion Parameters* (CRC Press, Boca Laton, FL, 1983).
  - <sup>35</sup> A. F. M. Barton, in *CRC Handbook of Solubility Parameters and Other Cohesion Parameters, 2nd edition*. (CRC Press, Boca Laton, FL, 1991).
  - <sup>36</sup> Y. Du, Y. Xue, and H. L. Frisch, in *AIP Handbook of Polymer Properties* (AIP Press, NY, 1996).
  - <sup>37</sup> O. Mishima and H. E. Stanley, Nature **396**, 329 (1998).
  - <sup>38</sup> A. Coccia, P. L. Indovina, F. Podo, and V. Viti, Chem. Phys. **7**, 30 (1975).
  - <sup>39</sup> K. Mizuno, T. Ochi, and Y. Shindo, J. Chem. Phys. **109**, 9502 (1998).
  - <sup>40</sup> K. Mizuno, s. Imafuji, T. Ochi, and S. Maeda, J. Phys. Chem. B **104**, 11001 (2000).
  - <sup>41</sup> C. L. Yaws, *Chemical Properties Handbook* (McGraw-Hill, New York, 1999).
  - <sup>42</sup> A. Barton, *Handbook of solubility parameters and other cohesion parameters* (CRC Press, Boca

Raton, 1991).

## Tables

TABLE I: Some parameters of the solvents: mass ( $M$ ), absolute mass difference to water ( $\Delta M$ ), radius of gyration ( $R_g$ ), z-component of the moment of inertia ( $I_{zz}$ ), dipole moment ( $\mu$ ), Hildebrandt parameter ( $\delta$ ),  $x_{\text{solvent}}^{\pm}$  the concentration when  $S_T = 0$  and the concentration  $x_{\text{solvent}}^{\text{hyd}}$ , where the hydrogen-bond network breaks down.

component	$M^{41}$ / a.m.u.	$\Delta M$ a.m.u.	$R_g^{41}$ / $\text{\AA}$	$\mu^{41}$ / Debye	$I_{zz}$ $\text{g}\cdot\text{\AA}^2/\text{Mol}$	$\delta^{42}$ $\text{MPa}^{1/2}$	$x_{\text{solvent}}^{\pm}$ at $S_T = 0$	$x_{\text{solvent}}^{\text{hyd}}$
water	18.02		0.615	1.85	1.71	47.9		
methanol	32.04	14.02	1.552	1.70	20.7	29.6	0.15	
ethanol	46.07	28.05	2.259	1.69	63.1	26.0	0.14	0.08 <sup>38</sup>
acetone	58.08	40.06	2.746	2.88	103.3	20.2	0.11	0.06 <sup>39</sup>
DMSO	78.13	60.11	2.840	3.96	120.6	24.5	0.20	0.10 <sup>40</sup>

## List of Figures

Figure 1: Refractive index  $n$  (a) and derivative of the refractive index ( $\partial n/\partial x$ ) (b) versus molar fraction of the organic solvents acetone (■, solid line) and DMSO (●, dashed line).

Figure 2: The refractive index increment with temperature ( $\partial n/\partial T$ ) versus the molar fraction of the organic solvents acetone (■) and DMSO (●).

Figure 3: Soret coefficient of (a) acetone (■) and (b) DMSO (●) as a function of the molar fraction of organic solvent. The solid symbols refer to TDFRS measurements and the corresponding open symbols represent simulation results.<sup>26</sup> The dashed line is a guide for the eyes.

Figure 4: Soret coefficient of methanol ( $\nabla$ ),<sup>16</sup> ethanol ( $\Delta$ ),<sup>29</sup> acetone (■) and DMSO (●) in water as function of the molar fraction of water.

figures

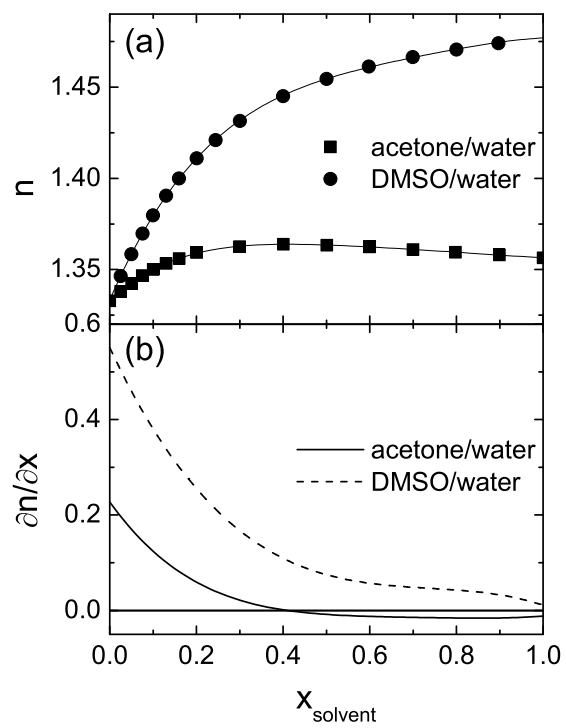


FIG. 1:

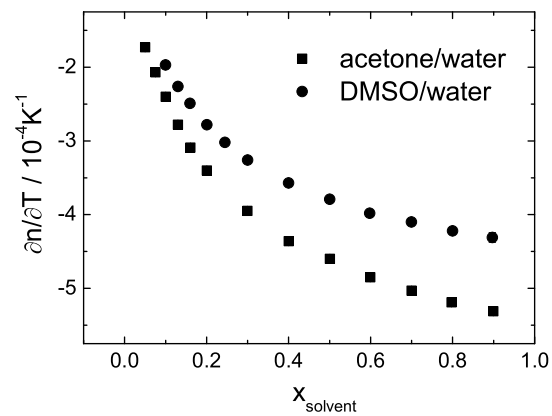


FIG. 2:

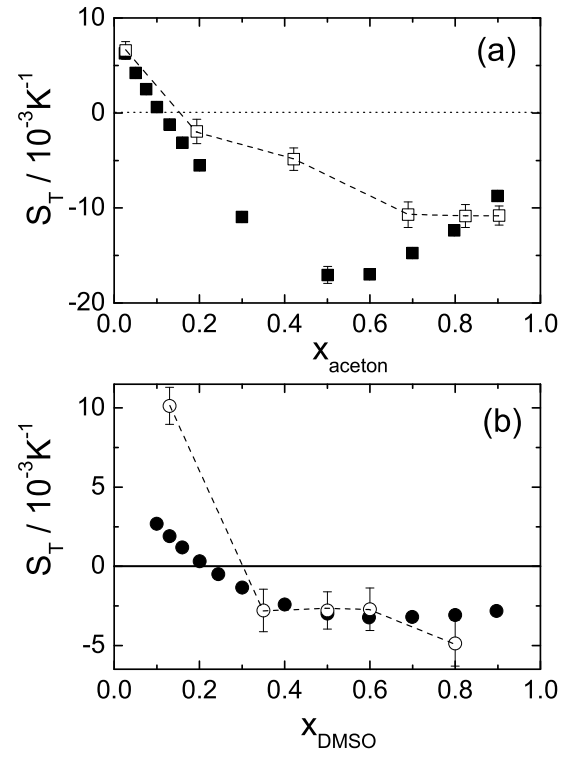


FIG. 3:

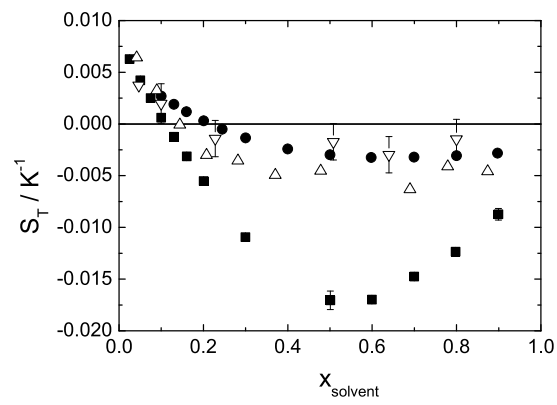


FIG. 4: